Structure of the Jahn-Teller–induced B absorption band of Tl^+-type centers in alkali halides

Akira Matsushima
Faculty of Liberal Arts, Nagasaki University, Bunkyo-cho, Nagasaki 852, Japan

Atsuo Fukuda
Department of Textile and Polymeric Materials, Tokyo Institute of Technology, Meguro-ku, Tokyo 152, Japan
(Received 5 April 1976)

The B- as well as A- and C-band shapes due to the electron-lattice interaction have been calculated systematically by using the Franck-Condon approximation. The linear electron-lattice interaction within the $a_{1g}t_{1u}$ excited states has been taken into consideration; it is written in terms of a 12×12 matrix by using the six interaction mode coordinates which belong to the α_{1g}, ϵ_g, and τ_{2g} irreducible representations of O_h group. The matrix has been diagonalized by the Givens-Householder method and the integration has been performed by the Monte Carlo method. The results can explain most of the characteristic features so far observed, indicating the validity of the Franck-Condon approximation and of the interaction mode coordinates even in the case of the Jahn-Teller–induced absorption band. An exception is the small peaks sometimes found in the middle part of the B band of Sn^{2+} center at very low temperatures (e.g., 4.2 K) which cannot be reproduced in the present calculation; the origin of these small peaks has been discussed. The effect of a magnetic field on the band shape (the magnetic circular dichroism shape) has also been calculated preliminarily.

I. INTRODUCTION

The transition $a_{1g}^2 \rightarrow a_{1g}t_{1u}$ in Tl^+-type centers with O_h symmetry produces three characteristic absorption bands called A, B, and C in order of increasing energy.[1] In most of these centers the electron-lattice interaction is so strong that the dynamic Jahn-Teller effect (JTE) causes the prominent structure of the A and C bands at high temperatures, which has been studied in detail as a typical example.[2-4] Toyozawa and Inoue,[5] Cho,[6] and Honma[7] calculated the band shapes of the A and C bands by using the classical Franck-Condon approximation, which can reproduce most of the observed characteristic features. Recently a more exact calculation was successfully performed by Nasu and Kojima[8] by using the independent ordering approximation.

Although the B band does not show any well-resolved structure at least at high temperatures, it is quite interesting to study the B band in more detail; as contrary to the A and C bands, the B band is due to the forbidden transitions and the absorption band itself is induced by the dynamic JTE. Band shapes of some Jahn-Teller induced absorption bands were studied theoretically by Kamimura and Yamaguchi[9] and also by Natsume,[10] but the transitions responsible for the B band are so complicated that its band shape is not analyzed by using their results. Tsuboi *et al.*[11] and Asano and Tomishina[12] calculated the B-band shape recently; their calculation is not satisfactory, however, because they oversimplified the effective Hamiltonian matrix representing the JTE.

We have been trying to calculate the B-band shape systematically. Some of the preliminary results were already published elsewhere.[13,14] In this paper will be given the detailed report on the calculated B-band shape, which can explain most of the observed characteristic features of the B band. We will also report some preliminary results of the calculated B-band magnetic-circular-dichroism (MCD) shape. Similar calculations have been made by Honma *et al.*[15] and Honma[16] who obtained the B-band shape together with its MCD shape by treating the effect of the A and C bands as perturbations. As will become clear in the following, however, the use of perturbation theory is not satisfactory in Sn^{2+} and Tl^+ centers. We have diagonalized the 12×12 matrix directly without using perturbation theory. Moreover we have chosen parameters in a way which makes easier the comparison of calculated results with experimental data.[17]

II. FORMULATION

We will consider two "active" electrons[18] which occupy the molecular orbitals around the center, a_{1g}^2 in the ground state and $a_{1g}t_{1u}$ in an excited state.[19] The total Hamiltonian is given by

$$\mathcal{H}=\mathcal{H}_0+\mathcal{H}_{ee}+\mathcal{H}_{so}+\mathcal{H}_z+\mathcal{H}_{eL}+\mathcal{H}_L\,, \tag{1}$$

where $\mathcal{H}_0$ is the kinetic energy of the two electrons plus their potential energy due to the central and surrounding ions located in the equilibrium lattice points, $\mathcal{H}_{ee}$ is the Coulomb repulsion energy between the two electrons, $\mathcal{H}_{so}$ is the spin-orbit interaction, $\mathcal{H}_z$ is the Zeeman energy when a magnetic field is applied, $\mathcal{H}_{eL}$ is the linear electron-lattice interaction, and $\mathcal{H}_L$ is the lattice kinetic

TABLE I. Matrix of the Zeeman interaction for a magnetic field, $\vec{H}=H_x\vec{i}+H_y\vec{j}+H_z\vec{k}$. Bases of the matrix are $|\Gamma_1^-\rangle$, $|\Gamma_4^-(^3T_{1u})\rangle$, $|\Gamma_3^-\rangle$, $|\Gamma_5^-\rangle$, and $|\Gamma_4^-(^1T_{1u})\rangle$. The orbital g factor is defined as follows: $\langle t_{1u,z}|l_x|t_{1u,y}\rangle=\langle t_{1u,x}|l_y|t_{1u,z}\rangle=\langle t_{1u,y}|l_z|t_{1u,x}\rangle=ig_{\rm orb}=ig$.

	$\lvert\Gamma_1^-\rangle$	$\lvert\Gamma_4^-(^3T_{1u})\rangle$			$\lvert\Gamma_3^-\rangle$		$\lvert\Gamma_5^-\rangle$		$\lvert\Gamma_4^-(^1T_{1u})\rangle$		
$\langle\Gamma_1^-\rvert$	0										
	$i\frac{\sqrt{2}}{\sqrt{3}}(2-g)\mu_B H_x$	0	$-i\frac{1}{\sqrt{2}}(2+g)\mu_B H_z$	$i\frac{1}{\sqrt{2}}(2+g)\mu_B H_y$							
$\langle\Gamma_4^-(^3T_{1u})\rvert$	$i\frac{\sqrt{2}}{\sqrt{3}}(2-g)\mu_B H_y$	$i\frac{1}{\sqrt{2}}(2+g)\mu_B H_z$	0	$-i\frac{1}{\sqrt{2}}(2+g)\mu_B H_x$							
	$i\frac{\sqrt{2}}{\sqrt{3}}(2-g)\mu_B H_z$	$-i\frac{1}{\sqrt{2}}(2+g)\mu_B H_y$	$i\frac{1}{\sqrt{2}}(2+g)\mu_B H_x$	0							
	0	$i\frac{1}{\sqrt{2}}(2-g)\mu_B H_x$	$-i\frac{1}{\sqrt{2}}(2-g)\mu_B H_y$	0	0	0	$i\frac{1}{\sqrt{2}}(2+g)\mu_B H_x$	$-i(2+g)\mu_B H_z$			
$\langle\Gamma_3^-\rvert$	0	$-i\frac{1}{2\sqrt{3}}(2-g)\mu_B H_x$	$-i\frac{1}{2\sqrt{3}}(2-g)\mu_B H_y$	$i\frac{1}{\sqrt{3}}(2-g)\mu_B H_z$	0	0	$i\frac{\sqrt{3}}{2}(2+g)\mu_B H_x$	$-i\frac{\sqrt{3}}{2}(2+g)\mu_B H_y$	0		
	0	0	$i\frac{1}{\sqrt{2}}(2-g)\mu_B H_z$	$i\frac{1}{\sqrt{2}}(2-g)\mu_B H_y$	$-i\frac{1}{\sqrt{2}}(2+g)\mu_B H_x$	$-i\frac{\sqrt{3}}{2}(2+g)\mu_B H_y$	0	$i\frac{1}{\sqrt{2}}(2+g)\mu_B H_z$	$-i\frac{1}{\sqrt{2}}(2+g)\mu_B H_y$		
$\langle\Gamma_5^-\rvert$	0	$i\frac{1}{\sqrt{2}}(2-g)\mu_B H_z$	0	$i\frac{1}{\sqrt{2}}(2-g)\mu_B H_x$	$-i\frac{1}{\sqrt{2}}(2+g)\mu_B H_y$	$i\frac{\sqrt{3}}{2}(2+g)\mu_B H_x$	$-i\frac{1}{\sqrt{2}}(2+g)\mu_B H_z$	0	$i\frac{1}{\sqrt{2}}(2+g)\mu_B H_x$		
	0	$i\frac{1}{\sqrt{2}}(2-g)\mu_B H_y$	$i\frac{1}{\sqrt{2}}(2-g)\mu_B H_x$	0	$i(2+g)\mu_B H_z$	0	$i\frac{1}{\sqrt{2}}(2+g)\mu_B H_y$	$-i\frac{1}{\sqrt{2}}(2+g)\mu_B H_x$	0		
	0	0	0	0	0	0	0	0	0	$-ig\mu_B H_z$	$ig\mu_B H_y$
$\langle\Gamma_4^-(^1T_{1u})\rvert$	0	0	0	0	0	0	0	0	$ig\mu_B H_z$	0	$-ig\mu_B H_x$
	0	0	0	0	0	0	0	0	$-ig\mu_B H_y$	$ig\mu_B H_x$	0

as well as potential energy. Since use is made of the Franck-Condon approximation, $\mathcal{H}_L$ will be neglected and the interaction mode coordinates will be used conveniently.[5] On the assumption that the $a_{1g}t_{1u}$ excited state is rather well separated from other excited states as well as the a_{1g}^2 ground state, we will calculate the band shape within the $a_{1g}t_{1u}$ excited state, disregarding $\mathcal{H}_0$. By choosing the basis functions, Γ_1^-, $\Gamma_4^-(^3T_{1u})$, Γ_3^-, Γ_5^-, and $\Gamma_4^-(^1T_{1u})$, the effective Hamiltonian matrices for $\mathcal{H}_{ee}+\mathcal{H}_{so}$, and $\mathcal{H}_{eL}$ are given in Tables VI and V of Ref. 20, and the matrix for $\mathcal{H}_z$ is given in Table I. Coulomb and exchange integrals F and G appear in $\mathcal{H}_{ee}$, a spin-orbit interaction parameter ζ and a King and Van Vleck's λ in $\mathcal{H}_{so}$, an orbital g factor $g_{\rm orb}$ and a magnetic field strength $\mu_B\vec{H}$ in $\mathcal{H}_z$, and three coupling constants a, b, and c with the α_{1g}, ϵ_g, τ_{2g} interaction modes in $\mathcal{H}_{eL}$. The Coulomb integral F does not play any role in determining the band shape in the present approximation, because F only shifts all the energy levels uniformly.

In order to make a general discussion on various Tl^+-type centers we normalize the energy by the separation between the C and A bands,

$$\Delta = E(\Gamma_4^-[C]) - E(\Gamma_4^-[A]), \tag{2}$$

and describe the $a_{1g}t_{1u}$ excited states in terms of the normalized B-band position,

$$x = \frac{E(\Gamma_3^- \text{ and } \Gamma_5^-) - E(\Gamma_4^-[A])}{\Delta} \tag{3}$$

and King and Van Vleck's λ.[17] Here $E(\Gamma_4^-[A])$, $E(\Gamma_3^-$ and $\Gamma_5^-)$, and $E(\Gamma_4^-[C])$ are the electronic positions of the A, B, and C bands which can be obtained by extrapolating their first moments to the absolute zero temperature; note that Γ_3^- and Γ_5^- are degenerate. The exchange integral and spin-orbit interaction parameter are given by

$$\frac{G}{\Delta} = -\frac{1+2\lambda^2}{2(2+\lambda^2)}\left(x-\tfrac{1}{2}\right) + \frac{3}{4(2+\lambda^2)}\left[1+2\lambda^2 x(1-x)\right]^{1/2}, \tag{4}$$

and

$$\frac{\zeta}{\Delta} = \frac{2}{2+\lambda^2}\left(x-\tfrac{1}{2}\right) + \frac{1}{2+\lambda^2}\left[1+2\lambda^2 x(1-x)\right]^{1/2}. \tag{5}$$

The energies of $\Gamma_4^-(^1T_{1u})$, $\Gamma_4^-(^3T_{1u})$, and Γ_1^- that appear in the diagonal part of the matrix for $\mathcal{H}_{ee}+\mathcal{H}_{so}$ are given by

$$\frac{E[\Gamma_4^-(^1T_{1u})] - E(\Gamma_4^-[A])}{\Delta} = \frac{1}{2} + \left(\frac{G}{\Delta} + \frac{1}{4}\frac{\zeta}{\Delta}\right), \tag{6}$$

$$\frac{E[\Gamma_4^-(^3T_{1u})] - E(\Gamma_4^-[A])}{\Delta} = \frac{1}{2} - \left(\frac{G}{\Delta} + \frac{1}{4}\frac{\zeta}{\Delta}\right), \tag{7}$$

and

$$\frac{E(\Gamma_1^-) - E(\Gamma_4^-[A])}{\Delta} = \frac{1}{2} - \frac{G}{\Delta} - \frac{3}{4}\frac{\xi}{\Delta}. \tag{8}$$

Note that $E(\Gamma_4^-[A])$ is taken as energy zero. In the actual calculations λ is set to be unity. Figure 1 shows how each of these energies changes as a function of x. The three coupling constants and the six interaction-mode coordinates are also made dimensionless accordingly, i.e.:

$$\frac{a}{\sqrt{\Delta}}, \quad \frac{b}{\sqrt{\Delta}}, \quad \frac{c}{\sqrt{\Delta}}, \tag{9}$$

and

$$\frac{\vec{Q}}{\sqrt{\Delta}}\left(\frac{Q_1}{\sqrt{\Delta}}, \frac{Q_2}{\sqrt{\Delta}}, \ldots, \frac{Q_6}{\sqrt{\Delta}}\right). \tag{10}$$

Putting

$$\epsilon = \frac{\hbar\omega - E(\Gamma_4^-[A])}{\Delta}, \tag{11}$$

we obtain the band-shape function

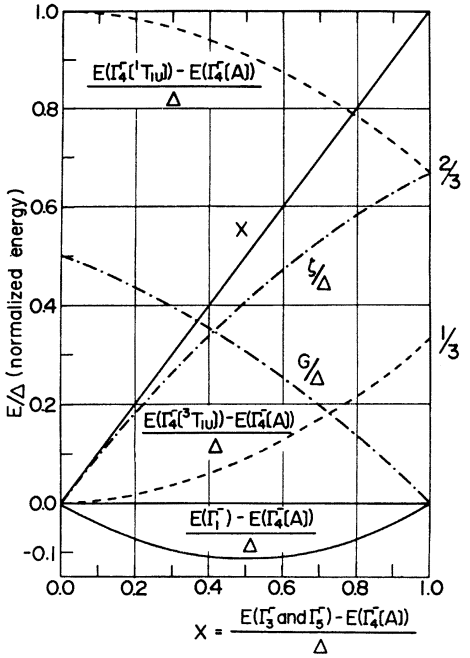

FIG. 1. Each of the energies, G/Δ, ξ/Δ, $\{E[\Gamma_4^-(^1T_{1u})] - E(\Gamma_4^-[A])\}/\Delta$, $\{E[\Gamma_4^-(^3T_{1u})] - E(\Gamma_4^-[A])\}/\Delta$, and $\{E(\Gamma_1^-) - E(\Gamma_4^-[A])\}/\Delta$ is plotted as a function of $x = \{E(\Gamma_3^- \text{ and } \Gamma_4^-) - E(\Gamma_4^-[A])\}/\Delta$, where $\Delta = E(\Gamma_4^-[C] - E(\Gamma_4^-[A])$.

$$f(\epsilon;\ x, a/\sqrt{\Delta}, b/\sqrt{\Delta}, c/\sqrt{\Delta}, kT/\Delta)$$

$$= \sum_{l=1}^{12} f^{(l)}$$

$$= \sum_{l=1}^{12} \int\int\cdots\int \left(\frac{1}{\pi kT/\Delta}\right)^3 \exp\left(-\frac{|\vec{Q}|^2/\Delta}{kT/\Delta}\right) |\langle e^{(l)}(\vec{Q}/\sqrt{\Delta}; x, a/\sqrt{\Delta}, b/\sqrt{\Delta}, c/\sqrt{\Delta})|M|g\rangle|^2$$

$$\times \delta(\epsilon - \epsilon^{(l)}(\vec{Q}/\sqrt{\Delta}; x, a/\sqrt{\Delta}, b/\sqrt{\Delta}, c/\sqrt{\Delta}))\ \frac{dQ_1 dQ_2 \cdots dQ_6}{\Delta^3}, \tag{12}$$

where M is the electric dipole operator. Here the $\epsilon^{(l)}$'s represent the eigenvalues of the matrix for $\mathcal{H}_{ee} + \mathcal{H}_{so} + \mathcal{H}_{eL}$ in order of increasing energy; the $\langle e^{(l)}|$'s are the corresponding eigenvectors and are given by

$$\langle e^{(l)}(\vec{Q}/\sqrt{\Delta};\ x, a/\sqrt{\Delta}, b/\sqrt{\Delta}, c/\sqrt{\Delta})| = c_1^{(l)}\langle\Gamma_1^-| + c_2^{(l)}\langle\Gamma_{4,x}^-(^3T_{1u})| + c_3^{(l)}\langle\Gamma_{4,y}^-(^3T_{1u})|$$

$$+ c_4^{(l)}\langle\Gamma_{4,z}^-(^3T_{1u})| + \cdots + c_{10}^{(l)}\langle\Gamma_{4,x}^-(^1T_{1u})| + c_{11}^{(l)}\langle\Gamma_{4,y}^-(^1T_{1u})| + c_{12}^{(l)}\langle\Gamma_{4,z}^-(^1T_{1u})|, \tag{13}$$

where the coefficients $c_i^{(l)}$ are functions of $\vec{Q}/\sqrt{\Delta}$ and parametrically depend on x, $a/\sqrt{\Delta}$, $b/\sqrt{\Delta}$, and $c/\sqrt{\Delta}$. The A-, B-, and C-band shapes are given by the sums,

$$\sum_{l=2}^{4} f^{(l)}, \quad \sum_{l=5}^{9} f^{(l)}, \quad \text{and} \quad \sum_{l=10}^{12} f^{(l)},$$

respectively, and $f^{(1)}$ is the band shape due to the transition $\Gamma_1^+ \rightarrow \Gamma_1^-$. Since the Tl^+-type center is of O_h symmetry, the band shape does not depend on the direction and the state of polarization of incident light. We have set $M = z$ and hence

$$|\langle e^{(l)}|M|g\rangle|^2 = |c_{12}^{(l)}|^2. \tag{14}$$

When a magnetic field is applied, the MCD shape

function

$$\Delta f(\epsilon;\ x, a/\sqrt{\Delta}, b/\sqrt{\Delta}, c/\sqrt{\Delta}, kT/\Delta, g_{\rm orb}, \mu_B\vec{H}/\Delta) = f_+ - f_- \quad (15)$$

is obtained by replacing the transition probability $|\langle e^{(I)}|M|g\rangle|^2$ in Eq. (12) with

$$|\langle e^{(I)}|M_+|g\rangle|^2 - |\langle e^{(I)}|M_-|g\rangle|^2, \quad (16)$$

where $M_\pm$ are the electric dipole operators for the transitions $\Delta M = \pm 1$, and by regarding $\epsilon^{(I)}$ and $\langle e^{(I)}|$ as respective eigenvalues and eigenvectors of the matrix for $\mathcal{H}_{ee}+\mathcal{H}_{\rm so}+\mathcal{H}_{eL}+\mathcal{H}_{\epsilon}$. The coefficients $c_i^{(I)}$'s parametrically depend on $g_{\rm orb}$ and $\mu_B\vec{H}/\Delta$ as well as x, $a/\sqrt{\Delta}$, $b/\sqrt{\Delta}$, and $c/\sqrt{\Delta}$. The A-, B-, and C-band MCD shapes are given by the sums,

$$\sum_{I=2}^{4}\Delta f^{(I)},\quad \sum_{I=5}^{9}\Delta f^{(I)},\quad \text{and}\quad \sum_{I=10}^{12}\Delta f^{(I)},$$

respectively, and $\Delta f^{(1)}$ represents the MCD shape of the band due to the transition $\Gamma_1^+ \to \Gamma_1^-$. Usually the magnetic field is applied along the [001] direction, i.e., $\vec{H}=H_z\vec{k}$ so that we have set

$$\begin{aligned}&|\langle e^{(I)}|M_+|g\rangle|^2 - |\langle e^{(I)}|M_-|g\rangle|^2\\ &= |\langle e^{(I)}|(x+iy)/\sqrt{2}\,|g\rangle|^2 - |\langle e^{(I)}|(x-iy)/\sqrt{2}\,|g\rangle|^2\\ &= 2[\mathrm{Re}(c_{10}^{(I)})\mathrm{Im}(c_{11}^{(I)}) - \mathrm{Im}(c_{10}^{(I)})\mathrm{Re}(c_{11}^{(I)})],\end{aligned} \quad (17)$$

where Re and Im indicate the respective real and imaginary parts of the $c_i^{(I)}$'s.

The actual integrations in Eqs. (12) and (15) concerning $dQ_2dQ_3\cdots dQ_6/(\Delta)^{5/2}$ were carried out by the Monte Carlo method[6] as follows: (a) Specify the parameter values, x, $b/\sqrt{\Delta}$, $c/\sqrt{\Delta}$, kT/Δ, $g_{\rm orb}$, and $\mu_B\vec{H}/\Delta$. (b) Produce one set of quasi-random numbers between -0.5 and 0.5 with Gaussian distribution

$$\left(\frac{1}{\pi kT}\right)^{1/2}\exp\left(-\frac{Q_i^2/\Delta}{kT/\Delta}\right)$$

for $Q_i/\sqrt{\Delta}$ $(i=2,3,\ldots,6)$.[6] (c) Define the matrix for $\mathcal{H}_{ee}+\mathcal{H}_{\rm so}+\mathcal{H}_{\epsilon}+\mathcal{H}_{eL}$ and diagonalize it to obtain the eigenvalues and eigenvectors by the Givens-Householder method.[21] (d) Calculate the transition probabilities given by Eqs. (14) and (17). (e) Divide the abscissa ϵ into unit cells at intervals of 0.01. (f) Find out to what cells the 12 eigenvalues belong and accumulate the transition probabilities found in Eqs. (14) and (17) in the corresponding cells. (g) Repeat the steps from (a) to (f) 7500 times. The obtained histogram is the band or MCD shapes for the transition $a_{1g}^2 \to a_{1g}t_{1u}$ with $a/\sqrt{\Delta}=0$. The integration concerning $dQ_1/\sqrt{\Delta}$ was performed by convolution.[5,6]

III. RESULTS

The τ_{2g} mode is expected to be most effective for the splitting of the B band[5]; we will first consider the case of $a/\sqrt{\Delta}=0$ and $b/\sqrt{\Delta}=0$. We set $c/\sqrt{\Delta}=1$, which is not unreasonable because of Table I of Ref. 17. The temperatures are chosen to be $kT/\Delta=0.01$ and 0.03, which correspond to about 100 and 300 K because Δ is known to be about 1 eV. In Fig. 2 are shown calculated results for $x=0.25$, 0.5, and 0.75, which represent approximately the In^+, Sn^{2+}, and Tl^+ centers, respectively.[17] The calculated results reproduce the several characteristic features of the A, B, and C bands already pointed out by previous investigators together with some new aspects: (i) The intensity of the A band increases as x; i.e., the spin-orbit interaction becomes large.[1,19] (ii) The width of the A, B, and C bands gets smaller as x increases.[5,19] (iii) The A band is doublet, and

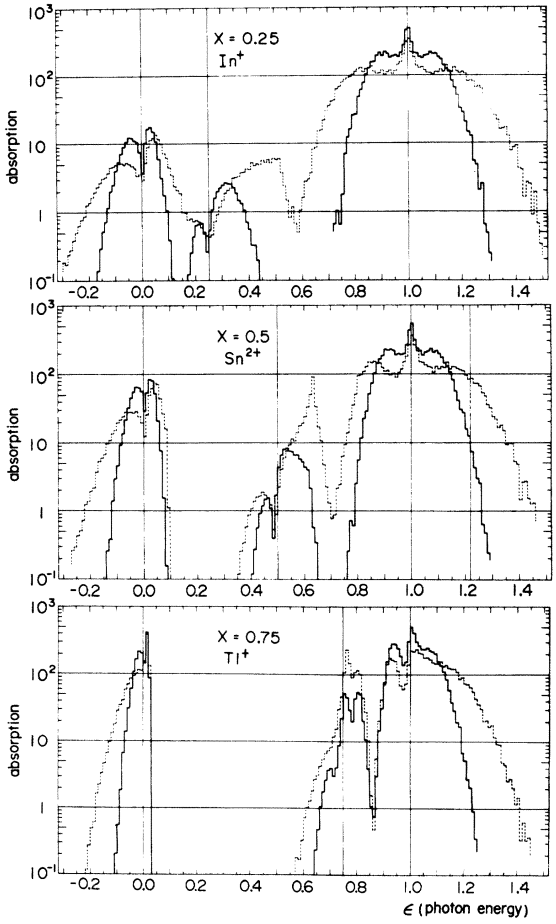

FIG. 2. Calculated band shapes for the $a_{1g}^2 \to a_{1g}t_{1u}$ transition. Coupling constants with the α_{1g}, ϵ_g, and τ_{2g} modes are set to be $a/\sqrt{\Delta}=0$, $b/\sqrt{\Delta}=0$, and $c/\sqrt{\Delta}=1$. Temperatures are $kT/\Delta=0.01$ (solid lines) and 0.03 (dotted lines).

the C band is triplet. The structure is enhanced with the increase of temperature.[1-8] (iv) The intensity of the B band increases with the rise of temperature.[1,19] (v) As the temperature increases, the first moment of the B band shifts toward the high-energy side when x is small, while it shifts toward the low-energy side when x is large.[19] (vi) The B band may be triplet, though the detailed structure depends strongly on x and the temperature. (vii) The smallest low-energy peak of the B band looks like a shoulder; its height relative to that of the central peak decreases as x increases. (viii) The band due to the transition $\Gamma_1^+ \rightarrow \Gamma_1^-$ cannot be observed. This is in accordance with Lemos *et al.*'s prediction[22] but in contradiction to Fowler's.[23]

We will next refer to the effect of the ϵ_g mode. When we put $a/\sqrt{\Delta}=0$, $b/\sqrt{\Delta}=1$, and $c/\sqrt{\Delta}=1$, we obtain Fig. 3; the additional coupling with the ϵ_g mode naturally increases the oscillator strength of the B band, but hardly changes the band shape. When we put $a/\sqrt{\Delta}=0$, $b/\sqrt{\Delta}=1$, and $c/\sqrt{\Delta}=0$, no splitting is observed in the calculated B-band shape as shown in Fig. 4. The oscillator strength of the B band in the case of $b/\sqrt{\Delta}=1$ and $c/\sqrt{\Delta}=0$ is smaller than that in the case of $b/\sqrt{\Delta}=0$ and $c/\sqrt{\Delta}=1$. In this way, the coupling with the τ_{2g} mode seems to be able to explain most of the observed characteristic features.

The adiabatic potential-energy surfaces responsible for the B band consist of five surfaces ($l=5$, 6, 7, 8, and 9). Transitions from the ground state to the lowest ($l=5$) and highest ($l=9$) surfaces are forbidden and hence do not contribute anything to the B band. The contribution to the B band of the transitions to the $l=6$, 7, and 8 surfaces is exemplified in Fig. 5 separately; the $l=6$ surface is responsible for the shoulder on the low-energy side.[13] In the case of the A and C bands, the transition to a particular surface

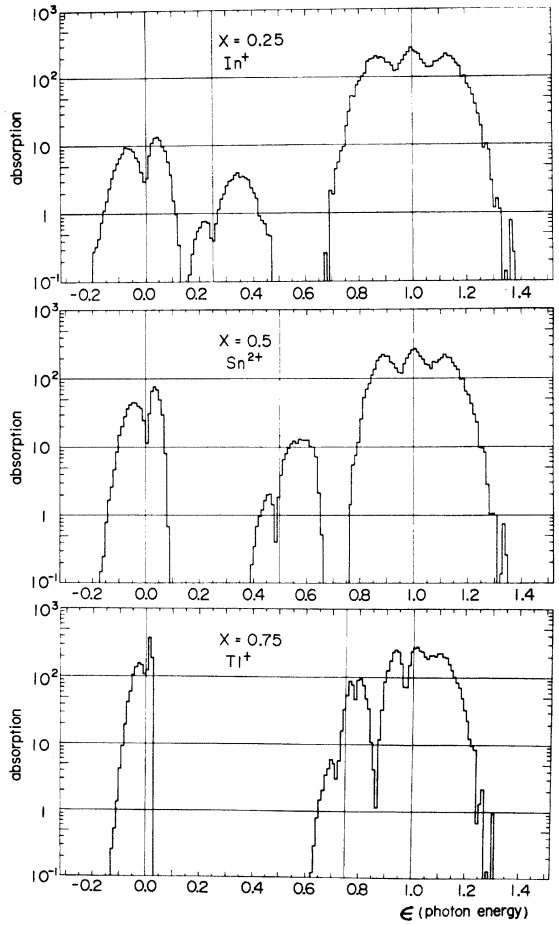

FIG. 3. Calculated band shapes for the $a_{1g}^2 \rightarrow a_{1g}t_{1u}$ transition. Coupling constants with α_{1g}, ϵ_g, and τ_{2g} modes are set to be $a/\sqrt{\Delta}=0$, $b/\sqrt{\Delta}=1$, and $c/\sqrt{\Delta}=1$. Temperature is $kT/\Delta=0.01$.

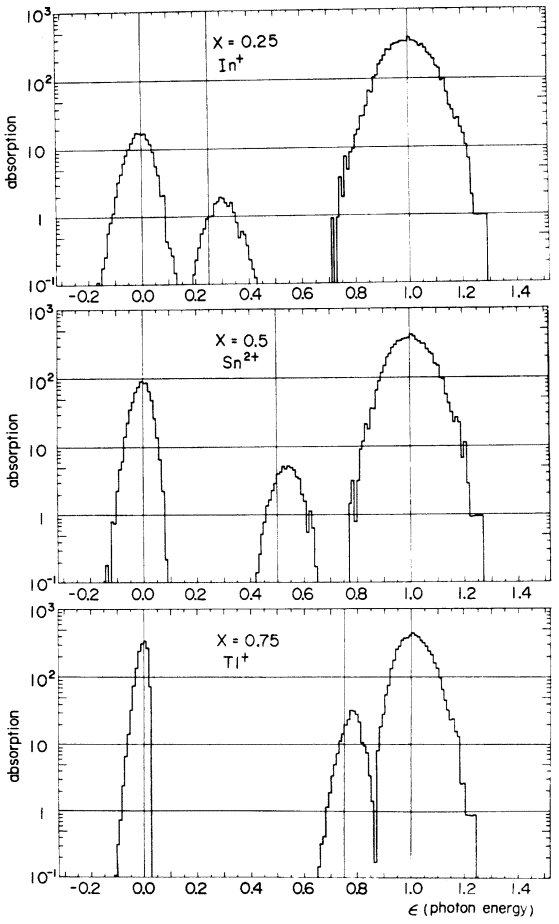

FIG. 4. Calculated band shapes for the $a_{1g}^2 \rightarrow a_{1g}t_{1u}$ transition. Coupling constants with the α_{1g}, ϵ_g, and τ_{2g} modes are set to be $a/\sqrt{\Delta}=0$, $b/\sqrt{\Delta}=1$, and $c/\sqrt{\Delta}=0$. Temperature is $kT/\Delta=0.01$.

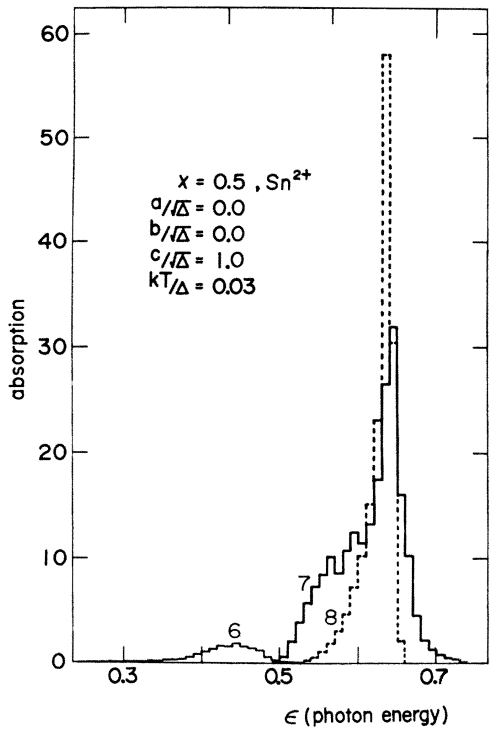

FIG. 5. Contributions to the B band of the transitions to the $l=6$, 7, and 8 surfaces.

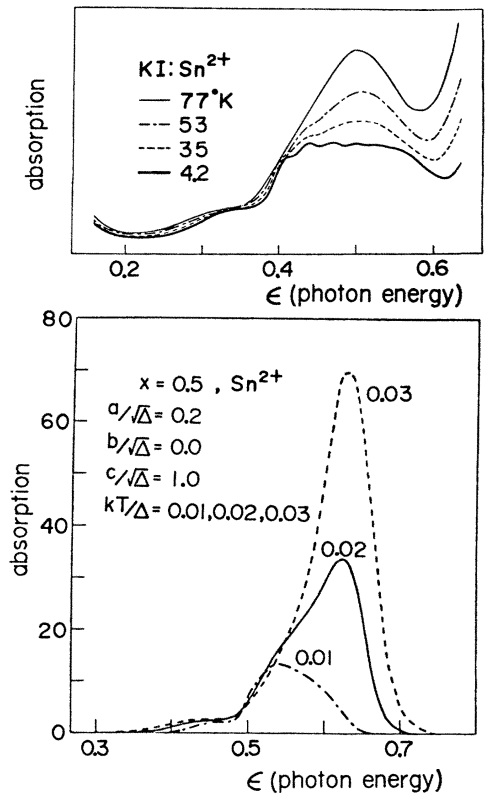

FIG. 6. Comparison between (a) the observed B band and (b) the calculated B-band shape in the case of $x=0.5$ (Sn^{2+}).

gives only one peak; hence the three peaks correspond to the three surfaces, though the two peaks overlap each other in the A band. In the case of the B band, however, the transition to a particular surface may give more than one peak; for example, the transition to the $l=7$ surface shows two peaks at about 0.58 and 0.63 as shown in Fig. 5.

Now let us consider whether the experimentally observed B-band structure can be explained by the calculated results. Since the detailed report for $x=0.25$ (In^+) has already been published elsewhere,[13] we will start with the case of $x=0.5$ (Sn^{2+}). Complex structure of the B band in the Sn^{2+} center was first noted in KI:Sn^{2+} by one of the authors[24] (A. F.) and was recently observed in KCl:Sn^{2+}, KBr:Sn^{2+}, RbCl:Sn^{2+}, and RbBr:Sn^{2+} as well as in KI:Sn^{2+} by Tsuboi *et al.*[25] and by Gannon and Jacobs.[26] Figure 6 (a) is the observed B band and Fig. 6(b) is the B-band shape calculated by using the not unreasonable parameter values cited in the figure. The coupling constant with the α_{1g} mode is expected to be small because the two active electrons are strongly attracted by the divalent Sn^{2+} ion.[5] Note the strong resemblance between Figs. 6 (a) and (b). Aside from the small peaks observed only at very low temperatures in the middle part of the B band in KI:Sn^{2+}, KBr:Sn^{2+}, and RbBr:Sn^{2+}, the calculated B-band shape can reproduce the characteristic triplet structure. A shoulder is clearly seen on the low-energy side even at rather high temperatures. At low temperatures the central peak is as high as the high-energy peak. As the temperature increases, the high-energy peak grows rapidly and the central peak becomes a shoulder. In KCl:Sn^{2+} and KBr:Sn^{2+}, for example, the high-energy peak is always higher than the central peak even at 4.2 K because of the large zero-point vibration. The origin of the aforementioned small peaks in the middle part of the B band will be discussed later.

We will next consider the case of $x=0.75$ (Tl^+). Figure 2 indicates that the B band of the Tl^+ center may have triplet structure. But detailed investigations so far made have not revealed any structure of the B band of the Tl^+ center.[27] Two reasons are probable: One is the fact that the height of the low-energy peak (shoulder) relative to that of the central peak (shoulder) decreases with the increase of x. The other is the fact that even a small coupling with the α_{1g} mode makes the structure indistinct as shown in Fig. 7.

Now let us consider the results of MCD shapes.

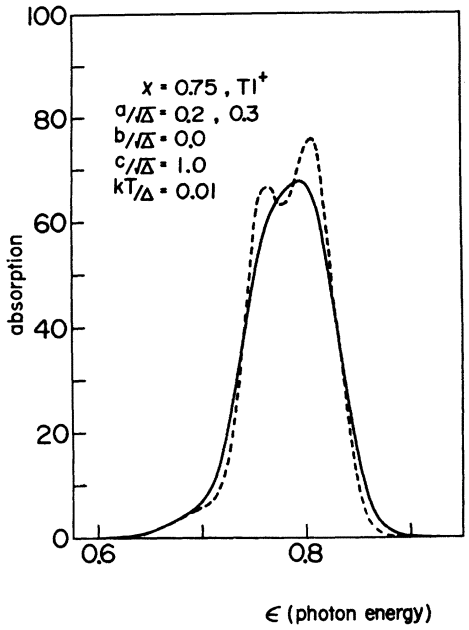

FIG. 7. Calculated B-band shape in the case of $x=0.75$ (Tl^+).

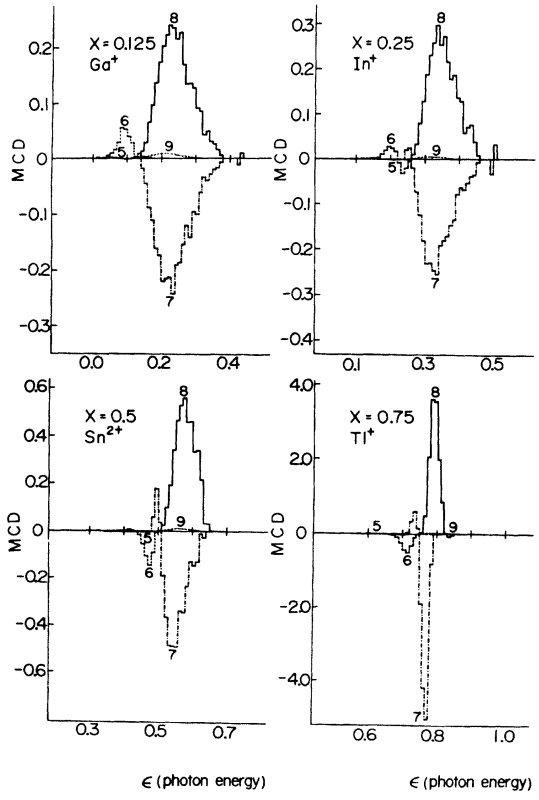

FIG. 8. Contributions to the B-band MCD of the transitions to $l=5$, 6, 7, 8, and 9 surfaces.

Since there are many parameters and morever since the calculation of the MCD shapes requires long central-processor-unit time, we have not yet performed systematic calculations. We only obtained the results for $a/\sqrt{\Delta}=0$, $b/\sqrt{\Delta}=0$, $c/\sqrt{\Delta}=1$, $KT/\Delta=0.01$, $g_{\rm orb}=1$, $\mu_B H_x/\Delta=0$, $\mu_B H_y/\Delta=0$, and $\mu_B H_z/\Delta=0.001$, which are shown in Fig. 8. The sets of random numbers used, 7500, are not enough for the calculation of the B-band MCD shape, though they give the rather nice A- and C-band MCD shapes as obtained previously by Cho.[6] In Fig. 8 are shown $\Delta f^{(l)}$ ($l=5$, 6, 7, 8, and 9) separately. Contributions of $\Delta f^{(5)}$ and $\Delta f^{(9)}$ are rather small, though not completely negligible as contrary to the case of the band shapes. Figure 8 indicates that the low-energy part of the MCD shape is determined by the transition to the $l=6$ surface of the Γ_3^- and Γ_5^- adiabatic potential-energy surfaces. When x is as small as $x=0.125$ and 0.25, the low-energy part gives a positive signal. When x is as large as 0.75, on the other hand, it gives a negative signal. The A-band MCD always gives the negative signal on the low-energy side. This tendency is experimentally observed in the Ga^+, In^+, and Tl^+ centers.[28,29]

IV. DISCUSSIONS

The results shown in Sec. III indicate the validity of the Franck-Condon approximation and of the interaction-mode coordinates. It should be noted, however, that the present calculation failed to reproduce the small peaks observed at very low temperatures in the middle part of the B band of $KI:Sn^{2+}$, $KBr:Sn^{2+}$, and $RbBr:Sn^{2+}$. This failure may be due to the inaccuracy of the Monte-Carlo integration performed. If we divide the energy scale more finely, say 0.001, and perform the Monte-Carlo integration more accurately by using more than 750 000 sets of random numbers, the result may be able to reproduce the small peaks; note that the transition to one surface can give more than one peak as pointed out in Sec. III. The reason for this failure might be more essential; the quantum-mechanical nature of lattice vibrations and/or the presence of a charge compensating vacancy might be responsible for these small peaks. It is also possible that the small peaks are due to some unknown centers which are different from a single Sn^{2+} ion associated with a charge-compensating vacancy.

The next problem is the asymmetry of the C band. Figures 2–4 indicate that the C-band shape tails to the high-energy side, while the experimentally observed C band tails to the low-energy side. If we take into account a quadratic effect, i.e., the difference in curvature between the

ground and excited states, we obtain the C-band shape tailing to the low-energy side.[7] Such a quadratic effect, however, will not change the B-band shape essentially. The difference in curvature is related to the fact that the $a_{1g}t_{1u}$ excited states are not isolated actually. The C-band MCD is very sensitive to this fact when the C band is located close to the D and exciton bands.[29] In such a case it is practically impossible to predict the C-band MCD shape without taking into consideration the effect of excited states other than $a_{1g}t_{1u}$.

In the calculation of the B-band MCD shape, $g_{\rm orb}$ should be chosen properly. In free Tl^+-type ions $g_{\rm orb}$ must be one. But according to Onaka *et al.*[30] the experimentally observed MCD indicates that $g_{\rm orb}$ is nearly quenched. Honma[16] calculated the B-band MCD shape by putting $g_{\rm orb}=0$ and showed that the MCD shape with $g_{\rm orb}=0$ is different from that with $g_{\rm orb}=1$. Unfortunately, however, they used perturbation theory, which is not good in the cases of $x=0.5$ and 0.75 as will become clear by comparing Figs. 2 and 3 with Fig. 2 of Ref. 15. It may not be reasonable to consider that the τ_{2g} mode is most effective in determining the B-band MCD shape, because Honma[31] insisted the importance of the coupling with the ϵ_g mode for the B-band MCD shape.

Before closing this discussion, we point out that both of the Γ_3^- and Γ_5^- are responsible for the B band. This conclusion is contrary to Bimberg *et al.*[32] that only the transition $\Gamma_1^+ \rightarrow \Gamma_5^-$ is responsible for the B band in KI:Tl^+. Their analysis entirely depends on an assumption that the B band is due to either of the transitions and not to the both. Since $\Gamma_3^- \times \Gamma_4^- = (\tau_{1g}) + \tau_{2g}$, and

$$\Gamma_5^- \times \Gamma_4^- = (\alpha_{2g}) + \epsilon_g + (\tau_{1g}) + \tau_{2g},$$

this assumption is unreasonable. Note that there is no interaction with the α_{2g} and τ_{1g} modes because of

$$(t_{1u} \times t_{1u})_{\rm sym} = \alpha_{1g} + \epsilon_g + \tau_{2g};$$

the electron-lattice interaction operates only on the orbital part of the wave functions, because the dependence of the spin-orbit interaction on lattice configuration is expected to be very small and hence is neglected.[5] In the similar way, the Lemos *et al.* prediction[22] that only $\Gamma_1^+ \rightarrow \Gamma_3^-$ is effective for the B band is also hard to understand.

ACKNOWLEDGMENTS

Numerical calculations were carried out by FACOM 230-75 at the Computer Center of Kyushu University. This work is partially supported by the Grant in Aid for Scientific Research from the Ministry of Education in Japan.

[1]W. B. Fowler, in *Physics of Color Centers*, edited by W. B. Fowler (Academic, New York, 1968), p. 133.
[2]A. Fukuda, J. Phys. Soc. Jpn. 27, 96 (1969). This contains an extensive bibliography before 1969.
[3]A. A. Braner and A. Halperin, Phys. Rev. B 4, 543 (1971).
[4]K. O. Gannon and P. W. M. Jacobs, J. Phys. Chem. Solids 36, 1383 (1975) and the references therein.
[5]Y. Toyozawa and M. Inoue, J. Phys. Soc. Jpn. 21, 1663 (1966).
[6]K. Cho, J. Phys. Soc. Jpn. 25, 1372 (1968).
[7]A. Honma, Sci. Light (Jpn.) 18, 33 (1969).
[8]K. Nasu and T. Kojima, Prog. Theor. Phys. 51, 26 (1974).
[9]H. Kamimura and T. Yamaguchi, J. Phys. Soc. Jpn. 25, 1138 (1968).
[10]Y. Natsume, Thesis (University of Tokyo, 1975) (unpublished).
[11]T. Tsuboi, Y. Nakai, K. Oyama, and P. W. M. Jacobs, Phys. Rev. B 8, 1698 (1973).
[12]S. Asano and Y. Tomishina, Research Laboratory for Surface Science, Okayama Univ. Report No. 4, (1973) (unpublished).
[13]A. Matsushima and A. Fukuda, Phys. Status Solidi B 66, 663 (1974).
[14]A. Matsushima and A. Fukuda, at International Conference on Color Centers in Ionic Crystals (Sendai, 1974) (unpublished) (Abstract No. 144).
[15]A. Honma, S. Ooaku, and T. Mabuchi, J. Phys. Soc. Jpn. 36, 1708 (1974).
[16]A. Honma, Sci. Light (Jpn.) 24, 33 (1975).
[17]A. Fukuda, K. Cho, and H. J. Paus, in *Luminescence of Crystals, Molecules, and Solutions*, edited by F. Williams (Plenum, New York, 1973), p. 478.
[18]M. D. Sturge, in *Solid State Physics*, edited by F. Seitz, D. Turnbull, and H. Ehrenreich (Academic, New York, 1967), Vol. 20, p. 109.
[19]A. Fukuda, Sci. Light (Jpn.) 13, 64 (1964).
[20]A. Fukuda, Phys. Rev. B 1, 4161 (1970).
[21]J. Ortega, in *Mathematical Methods for Digital Computers*, edited by A. Ralston and H. S. Wilf (Wiley, New York, 1957), Vol. 2, p. 94.
[22]A. M. Lemos, M. C. Stauber, and J. F. Marion, Phys. Rev. B 2, 4161 (1970).
[23]W. B. Fowler, Phys. Status Solidi 33, 763 (1969).
[24]A. Fukuda, Bussei (Maki-shoten, Jpn.) 10, 229 (1969).
[25]T. Tsuboi, K. Oyama, and P. W. M. Jacobs, J. Phys. C 7, 221 (1974).
[26]K. O. Gannon and P. W. M. Jacobs, J. Phys. Chem. Solids 36, 1375 (1975).
[27]T. Tsuboi and R. Kato, J. Phys. Soc. Jpn. 27, 1192 (1969).
[28]A. Fukuda and H. J. Paus (unpublished).
[29]T. Mabuchi (private communication).
[30]R. Onaka, T. Mabuchi, and A. Yoshikawa, J. Phys. Soc. Jpn. 23, 1036 (1967).
[31]A. Honma and S. Ooaku, J. Phys. Soc. Jpn. 41, 152 (1976).
[32]D. Bimberg, W. Dultz, and W. Gebhardt, Phys. Status Solidi 31, 661 (1969).